arXiv:1611.02797v1 [hep-ex] 9 Nov 2016

Observation of $\Lambda_c^+ \to nK_S^0\pi^+$

M. Ablikim[1], M. N. Achasov[9,e], S. Ahmed[14], X. C. Ai[1], O. Albayrak[5], M. Albrecht[4], D. J. Ambrose[44], A. Amoroso[49A,49C], F. F. An[1], Q. An[46,a], J. Z. Bai[1], O. Bakina[23], R. Baldini Ferroli[20A], Y. Ban[31], D. W. Bennett[19], J. V. Bennett[5], N. Berger[22], M. Bertani[20A], D. Bettoni[21A], J. M. Bian[43], F. Bianchi[49A,49C], E. Boger[23,c], I. Boyko[23], R. A. Briere[5], H. Cai[51], X. Cai[1,a], O. Cakir[40A], A. Calcaterra[20A], G. F. Cao[1], S. A. Cetin[40B], J. F. Chang[1,a], G. Chelkov[23,c,d], G. Chen[1], H. S. Chen[1], J. C. Chen[1], M. L. Chen[1,a], S. Chen[41], S. J. Chen[29], X. Chen[1,a], X. R. Chen[26], Y. B. Chen[1,a], X. K. Chu[31], G. Cibinetto[21A], H. L. Dai[1,a], J. P. Dai[34], A. Dbeyssi[14], D. Dedovich[23], Z. Y. Deng[1], A. Denig[22], I. Denysenko[23], M. Destefanis[49A,49C], F. De Mori[49A,49C], Y. Ding[27], C. Dong[30], J. Dong[1,a], L. Y. Dong[1], M. Y. Dong[1,a], Z. L. Dou[29], S. X. Du[53], P. F. Duan[1], J. Z. Fan[39], J. Fang[1,a], S. S. Fang[1], X. Fang[46,a], Y. Fang[1], R. Farinelli[21A,21B], L. Fava[49B,49C], F. Feldbauer[22], G. Felici[20A], C. Q. Feng[46,a], E. Fioravanti[21A], M. Fritsch[14,22], C. D. Fu[1], Q. Gao[1], X. L. Gao[46,a], Y. Gao[39], Z. Gao[46,a], I. Garzia[21A], K. Goetzen[10], L. Gong[30], W. X. Gong[1,a], W. Gradl[22], M. Greco[49A,49C], M. H. Gu[1,a], Y. T. Gu[12], Y. H. Guan[1], A. Q. Guo[1], L. B. Guo[28], R. P. Guo[1], Y. Guo[1], Y. P. Guo[22], Z. Haddadi[25], A. Hafner[22], S. Han[51], X. Q. Hao[15], F. A. Harris[42], K. L. He[1], F. H. Heinsius[4], T. Held[4], Y. K. Heng[1,a], T. Holtmann[4], Z. L. Hou[1], C. Hu[28], H. M. Hu[1], J. F. Hu[49A,49C], T. Hu[1,a], Y. Hu[1], G. S. Huang[46,a], J. S. Huang[15], X. T. Huang[33], X. Z. Huang[29], Z. L. Huang[27], T. Hussain[48], W. Ikegami Andersson[50], Q. Ji[1], Q. P. Ji[15], X. B. Ji[1], X. L. Ji[1,a], L. W. Jiang[51], X. S. Jiang[1,a], X. Y. Jiang[30], J. B. Jiao[33], Z. Jiao[17], D. P. Jin[1,a], S. Jin[1], T. Johansson[50], A. Julin[43], N. Kalantar-Nayestanaki[25], X. L. Kang[1], X. S. Kang[30], M. Kavatsyuk[25], B. C. Ke[5], P. Kiese[22], R. Kliemt[10], B. Kloss[22], O. B. Kolcu[40B,h], B. Kopf[4], M. Kornicer[42], A. Kupsc[50], W. Kühn[24], J. S. Lange[24], M. Lara[19], P. Larin[14], L. Lavezzi[49C,1], H. Leithoff[22], C. Leng[49C], C. Li[50], Cheng Li[46,a], D. M. Li[53], F. Li[1,a], F. Y. Li[31], G. Li[1], H. B. Li[1], H. J. Li[1], J. C. Li[1], Jin Li[32], K. Li[13], K. Li[33], Lei Li[3], P. R. Li[7,41], Q. Y. Li[33], T. Li[33], W. D. Li[1], W. G. Li[1], X. L. Li[33], X. N. Li[1,a], X. Q. Li[30], Y. B. Li[2], Z. B. Li[38], H. Liang[46,a], Y. F. Liang[36], Y. T. Liang[24], G. R. Liao[11], D. X. Lin[14], B. Liu[34], B. J. Liu[1], C. X. Liu[1], D. Liu[46,a], F. H. Liu[35], Fang Liu[1], Feng Liu[6], H. B. Liu[12], H. H. Liu[1], H. H. Liu[16], H. M. Liu[1], J. Liu[1], J. B. Liu[46,a], J. P. Liu[51], J. Y. Liu[1], K. Liu[39], K. Y. Liu[27], L. D. Liu[31], P. L. Liu[1,a], Q. Liu[41], Q. J. Liu[3], S. B. Liu[46,a], X. Liu[26], Y. B. Liu[30], Y. Y. Liu[30], Z. A. Liu[1,a], Z. Q. Liu[22], H. Loehner[25], X. C. Lou[1,a,g], H. J. Lu[17], J. G. Lu[1,a], Y. Lu[1], Y. P. Lu[1,a], C. L. Luo[28], M. X. Luo[52], T. Luo[42], X. L. Luo[1,a], X. R. Lyu[41], F. C. Ma[27], H. L. Ma[1], L. L. Ma[33], M. M. Ma[1], Q. M. Ma[1], T. Ma[1], X. N. Ma[30], X. Y. Ma[1,a], Y. M. Ma[33], F. E. Maas[14], M. Maggiora[49A,49C], Q. A. Malik[48], Y. J. Mao[31], Z. P. Mao[1], S. Marcello[49A,49C], J. G. Messchendorp[25], G. Mezzadri[21B], J. Min[1,a], T. J. Min[1], R. E. Mitchell[19], X. H. Mo[1,a], Y. J. Mo[6], C. Morales Morales[14], N. Yu. Muchnoi[9,e], H. Muramatsu[43], P. Musiol[4], Y. Nefedov[23], F. Nerling[10], I. B. Nikolaev[9,e], Z. Ning[1,a], S. Nisar[8], S. L. Niu[1,a], X. Y. Niu[1], S. L. Olsen[32], Q. Ouyang[1,a], S. Pacetti[20B], Y. Pan[46,a], P. Patteri[20A], M. Pelizaeus[4], H. P. Peng[46,a], K. Peters[10,i], J. Pettersson[50], J. L. Ping[28], R. G. Ping[1], R. Poling[43], V. Prasad[1], H. R. Qi[2], M. Qi[29], S. Qian[1,a], C. F. Qiao[41], L. Q. Qin[33], N. Qin[51], X. S. Qin[1], Z. H. Qin[1,a], J. F. Qiu[1], K. H. Rashid[48], C. F. Redmer[22], M. Ripka[22], G. Rong[1], Ch. Rosner[14], X. D. Ruan[12], A. Sarantsev[23,f], M. Savrié[21B], C. Schnier[4], K. Schoenning[50], W. Shan[31], M. Shao[46,a], C. P. Shen[2], P. X. Shen[30], X. Y. Shen[1], H. Y. Sheng[1], W. M. Song[1], X. Y. Song[1], S. Sosio[49A,49C], S. Spataro[49A,49C], G. X. Sun[1], J. F. Sun[15], S. S. Sun[1], X. H. Sun[1], Y. J. Sun[46,a], Y. Z. Sun[1], Z. J. Sun[1,a], Z. T. Sun[19], C. J. Tang[36], X. Tang[1], I. Tapan[40C], E. H. Thorndike[44], M. Tiemens[25], I. Uman[40D], G. S. Varner[42], B. Wang[30], B. L. Wang[41], D. Wang[31], D. Y. Wang[31], K. Wang[1,a], L. L. Wang[1], L. S. Wang[1], M. Wang[33], P. Wang[1], P. L. Wang[1], W. Wang[1,a], W. P. Wang[46,a], X. F. Wang[39], Y. Wang[37], Y. D. Wang[14], Y. F. Wang[1,a], Y. Q. Wang[22], Z. Wang[1,a], Z. G. Wang[1,a], Z. H. Wang[46,a], Z. Y. Wang[1], T. Weber[22], D. H. Wei[11], P. Weidenkaff[22], S. P. Wen[1], U. Wiedner[4], M. Wolke[50], L. H. Wu[1], L. J. Wu[1], Z. Wu[1,a], L. Xia[46,a], L. G. Xia[39], Y. Xia[18], D. Xiao[1], H. Xiao[47], Z. J. Xiao[28], Y. G. Xie[1,a], Yuehong Xie[6], Q. L. Xiu[1,a], G. F. Xu[1], J. J. Xu[1], L. Xu[1], Q. J. Xu[13], Q. N. Xu[41], X. P. Xu[37], L. Yan[49A,49C], W. B. Yan[46,a], W. C. Yan[46,a], Y. H. Yan[18], H. J. Yang[34,j], H. X. Yang[1], L. Yang[51], Y. X. Yang[11], M. Ye[1,a], M. H. Ye[7], J. H. Yin[1], Z. Y. You[38], B. X. Yu[1,a], C. X. Yu[30], J. S. Yu[26], C. Z. Yuan[1], Y. Yuan[1], A. Yuncu[40B,b], A. A. Zafar[48], Y. Zeng[18], Z. Zeng[46,a], B. X. Zhang[1], B. Y. Zhang[1,a], C. C. Zhang[1], D. H. Zhang[1], H. H. Zhang[38], H. Y. Zhang[1,a], J. Zhang[1], J. J. Zhang[1], J. L. Zhang[1], J. Q. Zhang[1], J. W. Zhang[1,a], J. Y. Zhang[1], J. Z. Zhang[1], K. Zhang[1], L. Zhang[1], S. Q. Zhang[30], X. Y. Zhang[33], Y. Zhang[1], Y. H. Zhang[1,a], Y. N. Zhang[41], Y. T. Zhang[46,a], Yu Zhang[41], Z. H. Zhang[6], Z. P. Zhang[46], Z. Y. Zhang[51], G. Zhao[1], J. W. Zhao[1,a], J. Y. Zhao[1], J. Z. Zhao[1,a], Lei Zhao[46,a], Ling Zhao[1], M. G. Zhao[30], Q. Zhao[1], Q. W. Zhao[1], S. J. Zhao[53], T. C. Zhao[1], Y. B. Zhao[1,a], Z. G. Zhao[46,a], A. Zhemchugov[23,c], B. Zheng[47], J. P. Zheng[1,a], W. J. Zheng[33], Y. H. Zheng[41], B. Zhong[28], L. Zhou[1,a], X. Zhou[51], X. K. Zhou[46,a], X. R. Zhou[46,a], X. Y. Zhou[1], K. Zhu[1], K. J. Zhu[1,a], S. Zhu[1], S. H. Zhu[45], X. L. Zhu[39], Y. C. Zhu[46,a], Y. S. Zhu[1], Z. A. Zhu[1], J. Zhuang[1,a], L. Zotti[49A,49C], B. S. Zou[1], J. H. Zou[1]

(BESIII Collaboration)

[1] *Institute of High Energy Physics, Beijing 100049, People's Republic of China*
[2] *Beihang University, Beijing 100191, People's Republic of China*
[3] *Beijing Institute of Petrochemical Technology, Beijing 102617, People's Republic of China*
[4] *Bochum Ruhr-University, D-44780 Bochum, Germany*
[5] *Carnegie Mellon University, Pittsburgh, Pennsylvania 15213, USA*
[6] *Central China Normal University, Wuhan 430079, People's Republic of China*
[7] *China Center of Advanced Science and Technology, Beijing 100190, People's Republic of China*
[8] *COMSATS Institute of Information Technology, Lahore, Defence Road, Off Raiwind Road, 54000 Lahore, Pakistan*
[9] *G.I. Budker Institute of Nuclear Physics SB RAS (BINP), Novosibirsk 630090, Russia*
[10] *GSI Helmholtzcentre for Heavy Ion Research GmbH, D-64291 Darmstadt, Germany*
[11] *Guangxi Normal University, Guilin 541004, People's Republic of China*

[12] Guangxi University, Nanning 530004, People's Republic of China
[13] Hangzhou Normal University, Hangzhou 310036, People's Republic of China
[14] Helmholtz Institute Mainz, Johann-Joachim-Becher-Weg 45, D-55099 Mainz, Germany
[15] Henan Normal University, Xinxiang 453007, People's Republic of China
[16] Henan University of Science and Technology, Luoyang 471003, People's Republic of China
[17] Huangshan College, Huangshan 245000, People's Republic of China
[18] Hunan University, Changsha 410082, People's Republic of China
[19] Indiana University, Bloomington, Indiana 47405, USA
[20] (A)INFN Laboratori Nazionali di Frascati, I-00044, Frascati, Italy; (B)INFN and University of Perugia, I-06100, Perugia, Italy
[21] (A)INFN Sezione di Ferrara, I-44122, Ferrara, Italy; (B)University of Ferrara, I-44122, Ferrara, Italy
[22] Johannes Gutenberg University of Mainz, Johann-Joachim-Becher-Weg 45, D-55099 Mainz, Germany
[23] Joint Institute for Nuclear Research, 141980 Dubna, Moscow region, Russia
[24] Justus-Liebig-Universitaet Giessen, II. Physikalisches Institut, Heinrich-Buff-Ring 16, D-35392 Giessen, Germany
[25] KVI-CART, University of Groningen, NL-9747 AA Groningen, The Netherlands
[26] Lanzhou University, Lanzhou 730000, People's Republic of China
[27] Liaoning University, Shenyang 110036, People's Republic of China
[28] Nanjing Normal University, Nanjing 210023, People's Republic of China
[29] Nanjing University, Nanjing 210093, People's Republic of China
[30] Nankai University, Tianjin 300071, People's Republic of China
[31] Peking University, Beijing 100871, People's Republic of China
[32] Seoul National University, Seoul, 151-747 Korea
[33] Shandong University, Jinan 250100, People's Republic of China
[34] Shanghai Jiao Tong University, Shanghai 200240, People's Republic of China
[35] Shanxi University, Taiyuan 030006, People's Republic of China
[36] Sichuan University, Chengdu 610064, People's Republic of China
[37] Soochow University, Suzhou 215006, People's Republic of China
[38] Sun Yat-Sen University, Guangzhou 510275, People's Republic of China
[39] Tsinghua University, Beijing 100084, People's Republic of China
[40] (A)Ankara University, 06100 Tandogan, Ankara, Turkey; (B)Istanbul Bilgi University, 34060 Eyup, Istanbul, Turkey; (C)Uludag University, 16059 Bursa, Turkey; (D)Near East University, Nicosia, North Cyprus, Mersin 10, Turkey
[41] University of Chinese Academy of Sciences, Beijing 100049, People's Republic of China
[42] University of Hawaii, Honolulu, Hawaii 96822, USA
[43] University of Minnesota, Minneapolis, Minnesota 55455, USA
[44] University of Rochester, Rochester, New York 14627, USA
[45] University of Science and Technology Liaoning, Anshan 114051, People's Republic of China
[46] University of Science and Technology of China, Hefei 230026, People's Republic of China
[47] University of South China, Hengyang 421001, People's Republic of China
[48] University of the Punjab, Lahore-54590, Pakistan
[49] (A)University of Turin, I-10125, Turin, Italy; (B)University of Eastern Piedmont, I-15121, Alessandria, Italy; (C)INFN, I-10125, Turin, Italy
[50] Uppsala University, Box 516, SE-75120 Uppsala, Sweden
[51] Wuhan University, Wuhan 430072, People's Republic of China
[52] Zhejiang University, Hangzhou 310027, People's Republic of China
[53] Zhengzhou University, Zhengzhou 450001, People's Republic of China

[a] Also at State Key Laboratory of Particle Detection and Electronics, Beijing 100049, Hefei 230026, People's Republic of China
[b] Also at Bogazici University, 34342 Istanbul, Turkey
[c] Also at the Moscow Institute of Physics and Technology, Moscow 141700, Russia
[d] Also at the Functional Electronics Laboratory, Tomsk State University, Tomsk, 634050, Russia
[e] Also at the Novosibirsk State University, Novosibirsk, 630090, Russia
[f] Also at the NRC "Kurchatov Institute", PNPI, 188300, Gatchina, Russia
[g] Also at University of Texas at Dallas, Richardson, Texas 75083, USA
[h] Also at Istanbul Arel University, 34295 Istanbul, Turkey
[i] Also at Goethe University Frankfurt, 60323 Frankfurt am Main, Germany
[j] Also at Institute of Nuclear and Particle Physics, Shanghai Key Laboratory for Particle Physics and Cosmology, Shanghai 200240, People's Republic of China

We report the first direct measurement of decays of the Λ_c^+ baryon involving the neutron. The analysis is performed using 567 pb^{-1} of e^+e^- collision data collected at $\sqrt{s} = 4.599$ GeV with the BESIII detector at the BEPCII collider. We observe the decay $\Lambda_c^+ \to nK_S^0\pi^+$ and measure the absolute branching fraction to be $\mathcal{B}(\Lambda_c^+ \to nK_S^0\pi^+) = (1.82 \pm 0.23(\text{stat}) \pm 0.11(\text{syst}))\%$. A comparison to $\mathcal{B}(\Lambda_c^+ \to p(\bar{K}\pi)^0)$ provides an important test of isospin symmetry and final state interactions.

PACS numbers: 13.30.Eg, 14.20.Lq, 13.66.Bc

The ground-state charmed baryon Λ_c^+ decays eventually into a proton or a neutron, each taking about half of the total branching fraction (BF) [1]. However, to date no direct measurement of the decay modes involving a neutron has been performed. It has been argued that isospin symmetry works well in the charmed baryon sector [2]. The relative BF of the neutron-involving decay to the proton-involving decay provides an important observable in testing isospin symmetry in Λ_c^+ decays. In addition, a measurement of the neutron mode helps to explore final state interactions [2]. The decay $\Lambda_c^+ \to n\bar{K}^0\pi^+$ is the most favored decay of the Λ_c involving a neutron. Hence, its comparison to the most favored proton mode $\Lambda_c^+ \to p(\bar{K}\pi)^0$ will allow a precise test on isospin symmetry and final state interactions. Throughout the paper, charge conjugate modes are always implied.

This Letter reports on the observation of the neutron-involving decay $\Lambda_c^+ \to nK_S^0\pi^+$. The data analyzed correspond to 567 pb^{-1} [3] of e^+e^- annihilations accumulated with the BESIII experiment at $\sqrt{s} = 4.599$ GeV [4]. This energy is slightly above the mass threshold of a $\Lambda_c^+\bar{\Lambda}_c^-$ pair, at which $\Lambda_c^+\bar{\Lambda}_c^-$ are produced in pairs and no additional hadron is kinematically allowed. The analysis technique in this work, which was first applied in the Mark III experiment [5], is specific for charm hadron pairs produced near threshold. First, we select a data sample of $\bar{\Lambda}_c^-$ baryons by reconstructing exclusive hadronic decays, called the single tag (ST) sample. Then, we search for $\Lambda_c^+ \to nK_S^0\pi^+$ in the system recoiling against the ST $\bar{\Lambda}_c^-$ baryons. In the final state $nK_S^0\pi^+$, the neutron is not detected, and its kinematics is deduced by four-momenta conservation. The absolute BF of $\Lambda_c^+ \to nK_S^0\pi^+$ is then determined from the probability of detecting the process $\Lambda_c^+ \to nK_S^0\pi^+$ in the ST sample. This method provides a clean and straightforward BF measurement independent of the total number of $\Lambda_c^+\bar{\Lambda}_c^-$ events produced.

The BESIII detector is a cylindrical detector with a solid-angle coverage of 93% of 4π that operates at the BEPCII collider. It consists of a Helium-gas based main drift chamber (MDC), a plastic scintillator time-of-flight (TOF) system, a CsI (Tl) electromagnetic calorimeter (EMC), a superconducting solenoid providing a 1.0 T magnetic field and a muon counter. The charged particle momentum resolution is 0.5% at a transverse momentum of 1 GeV/c. The photon energy resolution in EMC is 2.5% in the barrel and 5.0% in the end-caps at energies of 1 GeV. More details about the design and performance of the detector are given in Ref. [6].

A GEANT4-based [7] Monte Carlo (MC) simulation package, which includes a description of the detector geometry and the detector response, is used to determine the detection efficiency and to estimate potential backgrounds. Signal MC samples of a Λ_c^+ baryon decaying only to $nK_S^0\pi^+$ together with a $\bar{\Lambda}_c^-$ decaying only to the studied tag modes are generated by the MC event generator KKMC [8] using EVTGEN [9], including the effects of initial-state radiation (ISR) [10]. Final-state radiation (FSR) off the charged tracks is simulated with the PHOTOS package [11]. The $\Lambda_c^+ \to nK_S^0\pi^+$ decay is simulated using a phase space model since the two-body invariant mass spectra found in data for $M_{n\pi^+}$, $M_{nK_S^0}$ and $M_{K_S^0\pi^+}$ show no obvious structure. To study backgrounds, inclusive MC samples consisting of generic $\Lambda_c^+\bar{\Lambda}_c^-$ events, $D_{(s)}^{*}\bar{D}_{(s)}^{(*)} + X$ production, ISR return to the charmonium(-like) ψ states at lower masses, and QED processes are generated. All decay modes of the Λ_c, ψ and $D_{(s)}$ as specified in the Particle Data Group (PDG) [1] are simulated by the EVTGEN MC generator, while the unknown decays of the ψ states are generated with LUNDCHARM [12].

The ST $\bar{\Lambda}_c^-$ baryons are reconstructed using eleven hadronic decay modes as listed in the first column of Table I, where the intermediate particles K_S^0, $\bar{\Lambda}$, $\bar{\Sigma}^0$, $\bar{\Sigma}^-$ and π^0 are reconstructed through their decays of $K_S^0 \to \pi^+\pi^-$, $\bar{\Lambda} \to \bar{p}\pi^+$, $\bar{\Sigma}^0 \to \gamma\bar{\Lambda}$ with $\bar{\Lambda} \to \bar{p}\pi^+$, $\bar{\Sigma}^- \to \bar{p}\pi^0$ and $\pi^0 \to \gamma\gamma$, respectively.

Charged tracks are required to have polar angles within $|\cos\theta| < 0.93$, where θ is the polar angle of the charged track with respect to the beam direction. Their distances of closest approach to the interaction point (IP) are required to be less than 10 cm along the beam direction and less than 1 cm in the perpendicular plane. Tracks originating from K_S^0 and Λ decays are not subjected to these distance requirements. To discriminate pions from kaons, the specific ionization energy loss (dE/dx) in the MDC and TOF information are used to obtain particle identification (PID) probabilities for the pion ($\mathcal{L}_\pi$) and kaon ($\mathcal{L}_K$) hypotheses. Pion and kaon candidates are selected using $\mathcal{L}_\pi > \mathcal{L}_K$ and $\mathcal{L}_K > \mathcal{L}_\pi$, respectively. For proton identification, information from dE/dx, TOF, and EMC are combined to calculate the PID probability $\mathcal{L}'$, and a charged track satisfying $\mathcal{L}'_p > \mathcal{L}'_\pi$ and $\mathcal{L}'_p > \mathcal{L}'_K$ is identified as a proton candidate.

Photon candidates are reconstructed from isolated clusters in the EMC in the regions $|\cos\theta| \leq 0.80$ (barrel) and $0.86 \leq |\cos\theta| \leq 0.92$ (end cap). The deposited energy of a neutral cluster is required to be larger than 25 (50) MeV in barrel (end cap) region, and the angle between the photon candidate and the nearest charged track must be larger than 10°. To suppress electronic noise and energy deposits unrelated to the events, the difference between the EMC time and the event start time is required to be within (0, 700) ns. To reconstruct π^0 candidates, the invariant mass of the accepted photon pair is required to be within (0.110, 0.155) GeV/c^2. A kinematic fit is performed to constrain the $\gamma\gamma$ invariant mass to the nominal π^0 mass [1], and the χ^2 of the kinematic fit is required to be less than 20. The fitted momenta of the π^0 are used in the further analysis.

To reconstruct K_S^0 and $\bar{\Lambda}$ candidates, a vertex-

TABLE I. ST modes, ΔE requirements and ST yields $N_{\bar{\Lambda}_c^-}$ in data. The errors are statistical only.

Mode	ΔE (GeV)	$N_{\bar{\Lambda}_c^-}$
$\bar{p}K_S^0$	$[-0.025, 0.028]$	1066 ± 33
$\bar{p}K^+\pi^-$	$[-0.019, 0.023]$	5692 ± 88
$\bar{p}K_S^0\pi^0$	$[-0.035, 0.049]$	593 ± 41
$\bar{p}K^+\pi^-\pi^0$	$[-0.044, 0.052]$	1547 ± 61
$\bar{p}K_S^0\pi^+\pi^-$	$[-0.029, 0.032]$	516 ± 34
$\bar{\Lambda}\pi^-$	$[-0.033, 0.035]$	593 ± 25
$\bar{\Lambda}\pi^-\pi^0$	$[-0.037, 0.052]$	1864 ± 56
$\bar{\Lambda}\pi^-\pi^+\pi^-$	$[-0.028, 0.030]$	674 ± 36
$\bar{\Sigma}^0\pi^-$	$[-0.029, 0.032]$	532 ± 30
$\bar{\Sigma}^-\pi^0$	$[-0.038, 0.062]$	329 ± 28
$\bar{\Sigma}^-\pi^+\pi^-$	$[-0.049, 0.054]$	1009 ± 57

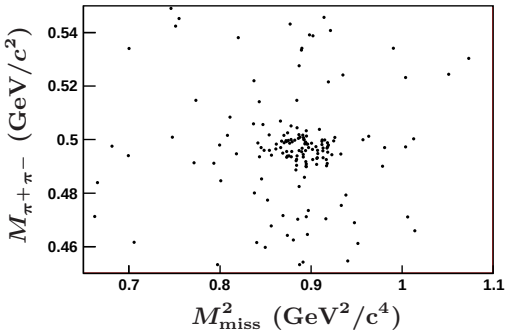

FIG. 1. Scatter plot of $M_{\pi^+\pi^-}$ versus $M^2_{\rm miss}$ for $\Lambda_c^+ \to nK_S^0\pi^+$ observed from data.

constrained fit is applied to $\pi^+\pi^-$ and $\bar{p}\pi^+$ combinations, and the fitted track parameters are used in the further analysis. The distance L of the secondary vertex to the IP is also required to be larger than zero. The same PID requirements as mentioned before are applied to the proton candidate, but not to the π candidate. The invariant masses $M_{\pi^+\pi^-}$, $M_{\bar{p}\pi^+}$, $M_{\gamma\bar{\Lambda}}$ and $M_{\bar{p}\pi^0}$ are required to be within (0.485, 0.510) GeV/c^2, (1.110, 1.121) GeV/c^2, (1.179, 1.205) GeV/c^2 and (1.173, 1.200) GeV/c^2 to select candidates for K_S^0, $\bar{\Lambda}$, $\bar{\Sigma}^0$ and $\bar{\Sigma}^-$ candidates, respectively.

For the ST mode $\bar{p}K_S^0\pi^0$, the backgrounds involving $\bar{\Lambda}$ and $\bar{\Sigma}^-$ are rejected by rejecting any event with $M_{\bar{p}\pi^+} \in (1.105, 1.125)\,\mathrm{GeV}/c^2$ and $M_{\bar{p}\pi^0} \in (1.173, 1.200)\,\mathrm{GeV}/c^2$. For the ST modes of $\bar{\Lambda}\pi^+\pi^-\pi^-$ and $\bar{\Sigma}^-\pi^+\pi^-$, the backgrounds involving K_S^0 and Λ as intermediate states are suppressed by requiring $M_{\pi^+\pi^-} \notin (0.480, 0.520)$ GeV/c^2 and $M_{\bar{p}\pi^+} \notin (1.105, 1.125)$ GeV/c^2.

The ST $\bar{\Lambda}_c^-$ signal candidates are identified using the beam constrained mass, $M_{\rm BC} \equiv \sqrt{E^2_{\rm beam} - |\overrightarrow{p}_{\bar{\Lambda}_c^-}|^2}$, where $E_{\rm beam}$ is the beam energy and $\overrightarrow{p}_{\bar{\Lambda}_c^-}$ is the momentum of the $\bar{\Lambda}_c^-$ candidate. To improve the signal purity, the energy difference $\Delta E \equiv E_{\rm beam} - E_{\bar{\Lambda}_c^-}$ for each candidate is required to be within approximately $\pm 3\sigma_{\Delta E}$ around the ΔE peak, where $\sigma_{\Delta E}$ is the ΔE resolution and $E_{\bar{\Lambda}_c^-}$ is the reconstructed $\bar{\Lambda}_c^-$ energy. The explicit ΔE requirements for the different modes are listed in Table I. The yield of each tag mode is obtained from fits to the $M_{\rm BC}$ distributions in the signal region $(2.280, 2.296)$ GeV/c^2, which is the same as in Ref. [13]. The yields of reconstructed singly tagged $\bar{\Lambda}_c^-$ baryons are listed in Table I. Finally, we obtain the total ST yield summed over all 11 modes to be $N^{\rm tot}_{\bar{\Lambda}_c^-} = 14415 \pm 159$, where the error is statistical only.

Candidates for the decay $\Lambda_c^+ \to nK_S^0\pi^+$ are selected from the remaining tracks recoiling against the ST $\bar{\Lambda}_c^-$ candidates. A pion with charge opposite to the ST $\bar{\Lambda}_c^-$ is selected, and a K_S^0 candidate is selected with the same selection criteria as described above but without the $M_{\pi^+\pi^-}$ mass requirement. If more than one K_S^0 candidate is formed, the one with the largest decay length significance L/σ_L is retained, where σ_L is the vertex resolution of L.

Since the neutron is not detected, we use a kinematic variable

$$M^2_{\rm miss} \equiv E^2_{\rm miss} - |\overrightarrow{p}_{\rm miss}|^2$$

to obtain information on the missing neutron, where $E_{\rm miss}$ and $\vec{p}_{\rm miss}$ are the missing energy and momentum carried by the neutron, respectively, which are calculated by $E_{\rm miss} \equiv E_{\rm beam} - E_{K_S^0} - E_{\pi^+}$ and $\vec{p}_{\rm miss} \equiv \vec{p}_{\Lambda_c^+} - \vec{p}_{K_S^0} - \vec{p}_{\pi^+}$, where $\vec{p}_{\Lambda_c^+}$ is the momentum of the Λ_c^+ baryon, $E_{K_S^0}$ ($\vec{p}_{K_S^0}$) and E_{π^+} ($\vec{p}_{\pi^+}$) are the energies (momenta) of the K_S^0 and π^+, respectively. Here, the momentum $\vec{p}_{\Lambda_c^+}$ is given by $\vec{p}_{\Lambda_c^+} = -\hat{p}_{\rm tag}\sqrt{E^2_{\rm beam} - m^2_{\bar{\Lambda}_c^-}}$, where $\hat{p}_{\rm tag}$ is the direction of the momentum of the ST $\bar{\Lambda}_c^-$ and $m_{\bar{\Lambda}_c^-}$ is the nominal $\bar{\Lambda}_c^-$ mass [1]. If the K_S^0 and π^+ from the decay $\Lambda_c^+ \to nK_S^0\pi^+$ are correctly identified, the $M^2_{\rm miss}$ is expected to peak around the nominal neutron mass squared.

The scatter plot of $M_{\pi^+\pi^-}$ versus $M^2_{\rm miss}$ for the $\Lambda_c^+ \to nK_S^0\pi^+$ candidates in data is shown in Fig. 1, where a cluster of events in the signal region is clearly visible. According to MC simulations, the dominant backgrounds are from the decays $\Lambda_c^+ \to \Sigma^-\pi^+\pi^+$ and $\Lambda_c^+ \to \Sigma^+\pi^+\pi^-$ with $\Sigma^\pm \to n\pi^\pm$, which have the same final state as signal. These background events form a peaking background in $M^2_{\rm miss}$, but are distributed flat in $M_{\pi^+\pi^-}$. Backgrounds from non-Λ_c^+ decays are estimated by examining the ST candidates in the M_{BC} sideband $(2.252, 2.272)$ GeV/c^2 in data, whose area is 1.6 times larger than the background area in the signal region.

To obtain the yield of $\Lambda_c^+ \to nK_S^0\pi^+$ events, we perform a two-dimensional unbinned maximum likelihood fit to the $M^2_{\rm miss}$ and $M_{\pi^+\pi^-}$ distributions in both $M_{\rm BC}$ signal and sideband regions simultaneously. As verified with MC simulations, we model the $M_{\pi^+\pi^-}$ and $M^2_{\rm miss}$ distributions with a product of two one-dimensional probability density functions (PDF), one for each dimension.

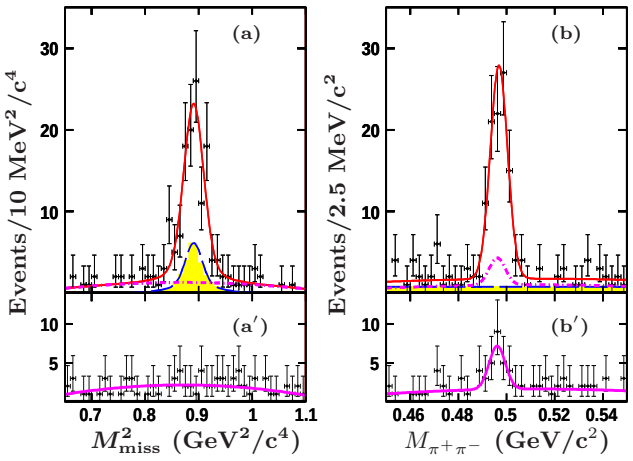

FIG. 2. Simultaneous fit to $M^2_{\rm miss}$ and $M_{\pi^+\pi^-}$ of events in (a, b) the $\bar{\Lambda}_c^-$ signal region and (a′, b′) sideband regions. Data are shown as the dots with error bars. The long-dashed lines (blue) show the Λ_c^+ backgrounds while the dot-dashed curves (pink) show the non-Λ_c^+ backgrounds. The (red) solid curves show the total fit. The (yellow) shaded area show the MC simulated backgrounds from Λ_c^+ decay.

The signal functions for $M^2_{\rm miss}$ and $M_{\pi^+\pi^-}$ are both described by double Gaussian functions. The peaking background in the $M^2_{\rm miss}$ distribution is described by a double Gaussian function with parameters fixed according to MC simulations, and the flat distribution in the $M_{\pi^+\pi^-}$ spectrum is described by a constant function. The non-Λ_c^+ decay background is modelled by a second-order polynomial function in the $M^2_{\rm miss}$ distribution and a Gaussian function plus a second-order polynomial function in the $M_{\pi^+\pi^-}$ distribution, in which the parameters and the normalized background yields are constrained by the events in $M_{\rm BC}$ sideband in the simultaneous fit. The fit procedure is validated by analyzing a large ensemble of MC-simulated samples, in which the pull distribution of the fitted yields is in good agreement with the normal distribution. Projections of the final fit to data are shown in Fig. 2. From the fit, we obtain $N^{\rm obs}_{nK^0_S\pi^+} = 83.2 \pm 10.6$, where the error is statistical only.

The absolute branching fraction for $\Lambda_c^+ \to nK^0_S\pi^+$ is determined by

$$\mathcal{B}(\Lambda_c^+ \to nK^0_S\pi^+) = \frac{N^{\rm obs}_{nK^0_S\pi^+}}{N^{\rm tot}_{\bar{\Lambda}_c^-} \times \varepsilon_{nK^0_S\pi^+} \times \mathcal{B}(K^0_S \to \pi^+\pi^-)}, \quad (1)$$

where $\varepsilon_{nK^0_S\pi^+}$ is the detection efficiency for the $\Lambda_c^+ \to nK^0_S\pi^+$ decay, which does not include the branching fraction for $K^0_S \to \pi^+\pi^-$. For each ST mode i, the efficiency $\epsilon^i_{nK^0_S\pi^+}$ is obtained by dividing the DT efficiency $\epsilon^i_{{\rm tag},nK^0_S\pi^+}$ by the ST efficiency $\epsilon^i_{\rm tag}$. Weighting $\epsilon^i_{nK^0_S\pi^+}$ by the ST yields in data for each tag mode, we obtain $\varepsilon_{nK^0_S\pi^+} = (45.9 \pm 0.3)\%$. Inserting the values of $N^{\rm obs}_{nK^0_S\pi^+}$, $N^{\rm tot}_{\bar{\Lambda}_c^-}$, $\varepsilon_{nK^0_S\pi^+}$ and $\mathcal{B}(K^0_S \to \pi^+\pi^-)$ [1] in Eq. (1), we obtain $\mathcal{B}(\Lambda_c^+ \to nK^0_S\pi^+) = (1.82 \pm 0.23)\%$, where the statistical error, including those from $N^{\rm obs}_{nK^0_S\pi^+}$ and $N^{\rm tot}_{\bar{\Lambda}_c^-}$ is presented.

TABLE II. Summary of the relative systematic uncertainties for $\mathcal{B}(\Lambda_c^+ \to nK^0_S\pi^+)$.

Source	Uncertainty
$\pi^\pm$ PID	1.0%
$\pi^\pm$ tracking	1.0%
K^0_S reconstruction	1.5%
Fit	5.2%
$\mathcal{B}(K^0_S \to \pi^+\pi^-)$	0.1%
$N^{\rm tot}_{\bar{\Lambda}_c^-}$	1.0%
MC statistics	0.6%
MC Model	1.3%
Total	5.9%

With the DT technique, the systematic uncertainties from the ST side cancel in the branching fraction measurement. The systematic uncertainties for measuring $\mathcal{B}(\Lambda_c^+ \to nK^0_S\pi^+)$ mainly arise from the uncertainties of PID, tracking, K^0_S reconstruction and the fit procedure. Throughout this paragraph, all quoted systematic uncertainties are relative uncertainties. The uncertainties in the π PID and tracking are both determined to be 1.0% by studying a set of control samples of $e^+e^- \to \pi^+\pi^-\pi^+\pi^-$, $e^+e^- \to K^+K^-\pi^+\pi^-$ and $e^+e^- \to p\bar{p}\pi^+\pi^-$ based on data taken at energies above 4.0 GeV. The uncertainty in the efficiency of K^0_S reconstruction is determined to be 1.5% by studying the control samples of $J/\psi \to K^{*\mp}K^\pm$ and $J/\psi \to \phi K^0_S K^\pm\pi^\mp$. The uncertainty due to the fit procedure is estimated to be 5.2% by varying the fit range, the shapes of background and signal components, and the choice of sideband regions. Besides these uncertainties mentioned above, there are systematic uncertainties from the quoted branching fraction for $K^0_S \to \pi^+\pi^-$ (0.1%), the $N^{\rm tot}_{\bar{\Lambda}_c^-}$ (1.0%) evaluated by using alternative signal shapes in fits to the $M_{\rm BC}$ spectra, the MC statistics (0.6%), the signal MC model (1.3%) estimated by taking into account the statistical variations in the $M_{n\pi^+}$, $M_{nK^0_S}$ and $M_{K^0_S\pi^+}$ spectra observed in data. These systematic uncertainties are summarized in Table II, and the total systematic error is estimated to be 5.9% by adding up all the sources in quadrature.

In summary, using 567 pb^{-1} of e^+e^- collision data taken at $\sqrt{s} = 4.599$ GeV with the BESIII detector, we report the observation of the decay $\Lambda_c^+ \to nK^0_S\pi^+$. We measure the absolute branching fraction for $\Lambda_c^+ \to nK^0_S\pi^+$, $\mathcal{B}(\Lambda_c^+ \to nK^0_S\pi^+) = (1.82 \pm 0.23 \pm 0.11)\%$, where the first error is statistical and the second systematic. This is the first direct measurement of a Λ_c^+ decay involving the neutron in the final state since the discovery of the Λ_c^+ more than 30 years ago. Using $\mathcal{B}(\Lambda_c^+ \to pK^-\pi^+)$

and $\mathcal{B}(\Lambda_c^+ \to pK_S^0\pi^0)$ measured at BESIII [14], we obtain $\mathcal{B}(\Lambda_c^+ \to n\bar{K}^0\pi^+)/\mathcal{B}(\Lambda_c^+ \to pK^-\pi^+) = 0.62 \pm 0.09$ and $\mathcal{B}(\Lambda_c^+ \to n\bar{K}^0\pi^+)/\mathcal{B}(\Lambda_c^+ \to p\bar{K}^0\pi^0)) = 0.97 \pm 0.16$ [15], in which the common uncertainties have been cancelled in the calculation. These ratios are useful to test the isospin symmetry and extract strong phases of different final states [2]. The measurement of the neutron mode in this work provides the first complementary data to the previously measured decays involving a proton, which represents significant progress in studying the Λ_c^+. The analysis method used in this work can also be extended to study more decay modes involving a neutron.

The BESIII collaboration thanks the staff of BEPCII and the IHEP computing center for their strong support. This work is supported in part by National Key Basic Research Program of China under Contract No. 2015CB856700; National Natural Science Foundation of China (NSFC) under Contracts Nos. 11235005, 11235011, 11305090, 11322544, 11305180, 11335008, 11425524, 11505010; the Chinese Academy of Sciences (CAS) Large-Scale Scientific Facility Program; the CAS Center for Excellence in Particle Physics (CCEPP); the Collaborative Innovation Center for Particles and Interactions (CICPI); Joint Large-Scale Scientific Facility Funds of the NSFC and CAS under Contracts Nos. U1232201, U1332201; CAS under Contracts Nos. KJCX2-YW-N29, KJCX2-YW-N45; 100 Talents Program of CAS; National 1000 Talents Program of China; INPAC and Shanghai Key Laboratory for Particle Physics and Cosmology; German Research Foundation DFG under Contracts Nos. Collaborative Research Center CRC 1044, FOR 2359; Istituto Nazionale di Fisica Nucleare, Italy; Joint Large-Scale Scientific Facility Funds of the NSFC and CAS under Contract No. U1532257; Joint Large-Scale Scientific Facility Funds of the NSFC and CAS under Contract No. U1532258; Koninklijke Nederlandse Akademie van Wetenschappen (KNAW) under Contract No. 530-4CDP03; Ministry of Development of Turkey under Contract No. DPT2006K-120470; NSFC under Contract No. 11275266; The Swedish Resarch Council; U. S. Department of Energy under Contracts Nos. DE-FG02-05ER41374, DE-SC-0010504, de-sc0012069, DESC0010118; U.S. National Science Foundation; University of Groningen (RuG) and the Helmholtzzentrum fuer Schwerionenforschung GmbH (GSI), Darmstadt; WCU Program of National Research Foundation of Korea under Contract No. R32-2008-000-10155-0. This paper is also supported by the Beijing municipal government under Contract Nos. KM201610017009, 2015000020124G064.

[1] K. A. Olive *et al.* [Particle Data Group], Chin. Phys. C **38**, 090001 (2014) and 2015 update.

[2] Cai-Dian Lü, Wei Wang and Fu-Sheng Yu, Phys. Rev. D **93**, 056008 (2016); H. Y. Cheng, Front. Phys. **10**(6), 101406 (2015); K. K. Sharma and R. C. Verma, Phys. Rev. D **55**, 7067 (1997); Ling-Lie Chau, Hai-Yang Cheng and B. Tseng, Phys. Rev. D **54**, 2132 (1996).

[3] M. Ablikim *et al.* [BESIII Collaboration], Chin. Phys. C **39**, 093001 (2015).

[4] M. Ablikim *et al.* [BESIII Collaboration], arXiv:1510.08654 [hep-ex].

[5] J. Adler *et al.* [Mark III Collaboration], Phys. Rev. Lett. **62**, 1821 (1989).

[6] M. Ablikim *et al.* [BESIII Collaboration], Nucl. Instrum. Meth. A **614**, 345 (2010).

[7] S. Agostinelli *et al.* [GEANT4 Collaboration], Nucl. Instrum. Meth. A **506**, 250 (2003).

[8] S. Jadach, B. F. L. Ward and Z. Was, Comput. Phys. Commun. **130**, 260 (2000); Phys. Rev. D **63**, 113009 (2001).

[9] D. J. Lange, Nucl. Instrum. Meth. A **462**, 152 (2001); R. G. Ping, Chin. Phys. C **32**, 599 (2008).

[10] E. A. Kurav and V. S. Fadin, Sov. J. Nucl. Phys. **41**, 466 (1985).

[11] E. Richter-Was, Phys. Lett. B **303**, 163 (1993); E. Barberio and Z. Was, Comput. Phys. Commun. **79**, 291 (1994).

[12] J. C. Chen, G. S. Huang, X. R. Qi, D. H. Zhang, Y. S. Zhu, Phys. Rev. D **62**, 034003 (2000).

[13] M. Ablikim *et al.* [BESIII Collaboration], Phys. Rev. Lett. **115**, 221805 (2015).

[14] M. Ablikim *et al.* [BESIII Collaboration], Phys. Rev. Lett. **116**, 052001 (2016).

[15] In the calculation, we assume that the processes with K_L^0 and K_S^0 included have the same branching fractions.